AS MS Journal of the American Society for
Mass Spectrometry

Research Article

Accelerated D-Fructose Acid-Catalyzed Reactions in Thin Films Formed by Charged Microdroplets Deposition

Chiara Salvitti,* Giulia de Petris, Anna Troiani, Marta Managò, Claudio Villani, Alessia Ciogli, Andrea Sorato, Andreina Ricci, and Federico Pepi*

Cite This: https://doi.org/10.1021/jasms.1c00363

Read Online

ACCESS | 📊 Metrics & More | 📖 Article Recommendations | SI Supporting Information

ABSTRACT: Thin films derived by the deposition of charged microdroplets generated in the ESI source of a mass spectrometer act as highly concentrated reaction vessels in which the final products of an ion–molecule reaction can be isolated by their precipitation onto a solid surface under ambient conditions. In this study, the ESI Z-spray source supplied to a Q-TOF Ultima mass spectrometer was used to investigate the D-fructose acid-catalyzed reactions by microdroplets deposition onto a stainless-steel target surface. High conversion ratios of D-fructose into 5-hydroxymethylfuraldehyde (5-HMF), 5-methoxymethylfuraldehyde (5-MMF), and difructose anhydrides (DFAs) were obtained with HCl and $KHSO_4$ as metal-free catalysts by using synthetic conditions under which the same products in bulk are not formed. Furthermore, the reaction outcome was found to be highly sensitive to the catalyst and the solvent employed as well as to the ESI source parameters influencing the thin film formation from microdroplets deposition onto the solid surface.

REACTION ACCELERATION

ESI probe

Δ N_2

- ve | + ve

Reaction products

D-Fructose solution

[%]

m/z

KEYWORDS: microdroplets, thin film, D-fructose, dehydration, methylation, dimerization
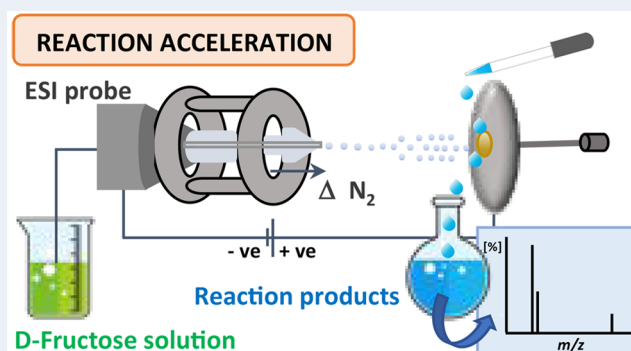
INTRODUCTION

In addition to its use as an analytical tool, mass spectrometry (MS) has long been employed in reaction monitoring to intercept elusive intermediates and highlight the mechanistic details of a chemical transformation.[1−6] The introduction of electrospray ionization (ESI) by Fenn et al.[7] enables one to directly generate a plume of charged microdroplets from a diluted aliquot of a reaction mixture. Once desolvated, the microdroplets release isolated ionic species that provide an accurate picture of the reaction progress in solution. Moreover, by increasing the distance between the ESI source and the MS entrance, the desolvation time of the charged droplets in the air increases. As a consequence, the ionized reagents, typically detected by MS at short distances, may be replaced by the reaction intermediates or even by the reaction final products. In the confined volume of the microdroplets, the reaction rate can be accelerated up to 10^5 times compared to the same process occurring in bulk[8] becoming comparable to that measured in the gas phase where the reactivity of the reactants is not influenced by the solvent molecules. Nevertheless, gas-phase reactions can be fast, but in most cases, they do not produce enough product for practical applications.[9−11] Conversely, under suitable conditions, the charged microdroplets generated in the ESI source may act as small reaction vessels in which the final products of an ion–molecule reaction can be easily isolated by their deposition onto a solid

surface.[12−20] The microdroplets landing onto the solid surface continuously generate a thin film that is characterized by a longer lifetime with respect to the microdroplets but retains their peculiar confined volume needed for reaction acceleration.[13,21,22]

Since several milestone reactions of organic chemistry have been recently accelerated in the microdroplets/thin films environment,[23] we decide to extend our studies about the decomposition of sugars in the gas phase[24−28] to the confined volumes of the microdroplets/thin films systems in an attempt to scale up this procedure for potential synthetic applications.

Processes allowing the utilization of carbohydrates from lignocellulosic biomass as a renewable resource have received great attention over time. Furan derivatives, such as 5-hydroxymethylfuraldehyde (5-HMF), are produced by the acid-catalyzed dehydration of hexoses, thus obtaining key-building block molecules from "green" resources.[29−33] In water solutions, the reaction is conducted at high temperatures and catalyzed by strong inorganic acids. The highest 5-HMF yields

A

66 were obtained from D-fructose, although the reaction in bulk
67 presents numerous drawbacks that limited its industrial
68 application, such as the rapid hydrolyses of 5-HMF to levulinic
69 acid or the formation of insoluble humins.

70   An additional important reaction observed in D-fructose
71 acidic solutions is the condensation of two D-fructose
72 molecules leading to the formation of difructose anhydrides
73 (DFAs) by the loss of water.[34−36] DFAs are a group of
74 isomeric oligosaccharides that can be used as low-calorie
75 sweeteners.[37] Important probiotic properties have been
76 recently attributed to this class of compounds, such as
77 promoting the growth of beneficial microflora in the gut and
78 protecting the intestinal tract favoring the assimilation of
79 antioxidants.[38]

80   Dehydration and dimerization represent the two different
81 reaction channels characteristic of the D-fructose carameliza-
82 tion under acidic conditions. In solution, the fructosylox-
83 ocarbenium cation (m/z 163), arising from the first
84 dehydration of D-fructose, can alternatively dehydrate to
85 produce 5-HMF or dimerize and cyclize to produce DFAs
86 (Scheme 1).

s1

Scheme 1. Mechanistic Pathway of the Acid-Catalyzed Caramelization of D-Fructose in Bulk[a]
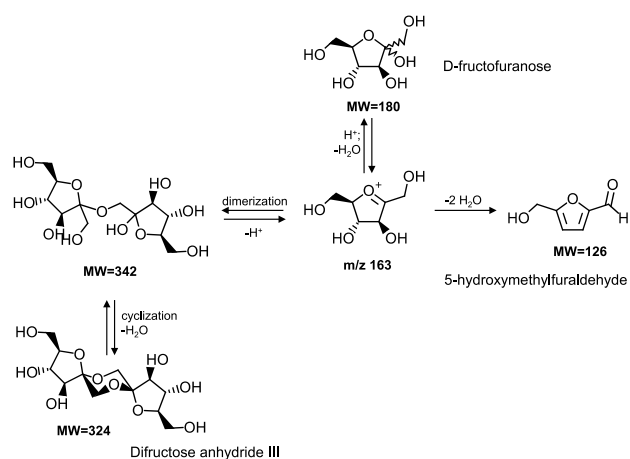
[a]The dimerization/cyclization reaction showed involves the same C1-OH groups of two D-fructose molecules leading to difructose anhydride III.

87   In this study, the D-fructose acid-catalyzed reactions in the
88 microdroplets/thin-film systems were investigated by using the
89 ESI Z-spray source of a Q-TOF mass spectrometer recently
90 adapted to perform ion and microdroplet deposition experi-
91 ments.[39] Different solvent mixtures containing HCl and
92 KHSO$_4$ as acid catalysts were used. Strong inorganic acids,
93 such as hydrochloric acid, are commonly used in the hexose
94 dehydration/dimerization reactions in water, whereas KHSO$_4$
95 has been recently recognized as a selective and safe acid
96 catalyst for sugar conversion to 5-HMF.[40] The efficiencies of
97 the observed reactions were evaluated in terms of conversion
98 ratio (CR) and apparent acceleration factor (AAF) with
99 respect to the same process in bulk. The branching ratios of
100 the different reaction channels were evaluated as a function of
101 the catalysts and solvents employed, as well as of the ESI
102 source parameters used.

■ EXPERIMENTAL SECTION

103

Reagents. D-fructose, 5-HMF, 5-MMF, HCl, KHSO$_4$, 104
solvents, and all other chemicals were purchased from 105
Sigma-Aldrich Ltd. and used without further purification. 106

Mass Spectrometric Experiments. Microdroplet deposi- 107
tion experiments were performed by using the Z-spray ESI 108
source of a quadrupole-time-of-flight (Q-TOF) mass spec- 109
trometer (Micromass, Manchester, UK) suitably adapted to 110
microdroplets reaction studies and operating in positive-ion 111
mode. 112

D-Fructose and the catalyst (HCl or KHSO$_4$) were dissolved 113
in H$_2$O or CH$_3$OH/H$_2$O and CH$_3$CN/H$_2$O mixtures to 114
millimolar concentrations, electrosprayed into the ESI source 115
of the instrument, and online analyzed before the micro- 116
droplets deposition experiments. Nitrogen was used as 117
desolvation gas at a flow rate of 200 L h^{-1}, whereas source 118
and desolvation temperatures were set at 80 and 200 °C, 119
respectively. Typical source potentials are as follows: capillary 120
4 kV, cone 60 V, RF lens-1 70 V, and syringe pump flow 20 μL 121
min^{-1}. According to the experimental procedure adopted in 122
this study, after acquiring the zero-time mass spectrum of the 123
solution in the 50−500 m/z range, 1 mL of the same mixture 124
was infused into the ESI source and the charged microdroplets 125
were collected onto a stainless-steel plate held 3.0 cm away 126
from the capillary tip. 127

A total reaction time of 50 min can be estimated by 128
considering the solution volume of 1 mL infused at a rate of 20 129
μL min^{-1}. Microdroplet deposition leads to the formation of a 130
solid precipitate that was rinsed with 1 mL of the same sprayed 131
solvents mixture, and the resulting solution was mass-analyzed 132
under the same ESI experimental conditions used to acquire 133
the zero-time mass spectrum. The amount of the collected 134
solid precipitate was measured by depositing the microdroplets 135
onto a previously weighed portion of aluminum foil. 136
Depending on the spray temperature used, the solid recovery 137
in the HCl-containing solutions varied from 90% at low 138
temperatures (the solid mainly contains unreacted D-fructose) 139
to 60−70% at spray temperatures around 150 °C. The same 140
estimation was critical in the KHSO$_4$ systems since this salt is 141
hygroscopic and sometimes the amount of the collected mass 142
was higher than the starting one. 143

The reactions were also performed in bulk by heating the 144
starting solutions of D-fructose containing HCl or KHSO$_4$ at 145
100 °C for 1 h under reflux. After this time, the reaction 146
mixture was quenched, cooled, and analyzed by mass 147
spectrometry. 148

The reaction progress has been qualitatively evaluated by 149
measuring the conversion ratio (CR) following the general 150
formula [P1]/([R] + [I] + [P1] + [P2]) where P1 is the ionic 151
intensity of the microdroplets product, whereas [R], [I], and 152
[P2] are the ionic intensities of the reagent, intermediates, and 153
reaction byproducts, respectively. The intensity of the ions was 154
processed without any correction due to different ionization 155
efficiencies. Changes in the conversion ratios were in turn 156
evaluated as a function of the source parameters by varying the 157
capillary voltage (0−4 kV), the desolvation temperature (50− 158
350 °C), and the capillary tip-stainless steel plate distance 159
(0.5−3.0 cm). 160

The apparent acceleration factors (AAF) of the reactions 161
were obtained by comparing the intensity ratio between 162
products and reagents from the droplets deposition process to 163

164 the corresponding value measured for the reaction in bulk
165 according to the equation $([P]/[R])_{droplet}/([P]/[R])_{bulk}$.
166   The reaction products and intermediates were characterized
167 by collision-induced dissociation (CID) experiments. CID
168 mass spectra were acquired by introducing Ar as the target gas
169 into the quadrupole cell at pressures of about 0.1−0.5 mTorr.
170 Data acquisition and processing were carried out by using the
171 MassLynx version 4.0 software supplied with the instrument.

■ RESULTS AND DISCUSSION

173 To investigate the acid-catalyzed hexose sugar reactivity by
174 microdroplets deposition, D-fructose solutions with variable
175 content of HCl and KHSO$_4$ were sprayed into the ESI Z-spray
176 source of a Q-TOF mass spectrometer recently adapted to
177 perform microdroplets reactivity experiments.[39] The stability
178 of the D-fructose acidic solutions at 25 °C was first evaluated
179 by analyzing the starting mixtures. No sugar decomposition
180 was observed at pH = 3 for both the HCl and KHSO$_4$ systems
181 even after several days from their preparation, whereas at lower
182 pH values an increasing decomposition of the sugar even at 25
183 °C was observed especially with HCl. Thus, the D-fructose
184 reactivity was studied by using solutions having pH values ≥ 3.
185 The microdroplets generated by the ESI source were collected
186 onto a stainless-steel plate placed in front of the ESI capillary.
187 After the microdroplets deposition, a white or brown solid
188 residue was formed on the metal surface depending on the
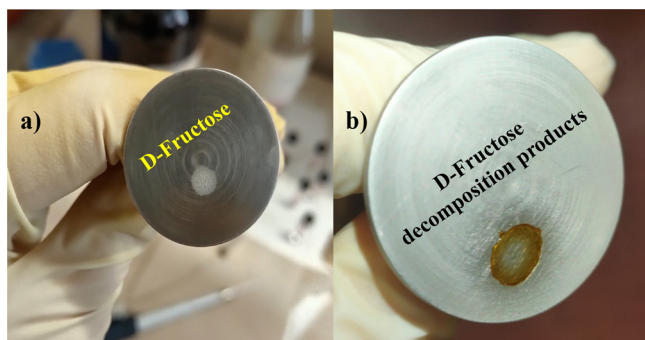189 source parameters used (Figure 1).

Figure 1. Solid residues recovered after microdroplet deposition: (a) white D-fructose crystals; (b) brown solid containing a mixture of D-fructose decomposition products.

190   The solid was then rinsed with the same sprayed solvent
191 mixture and analyzed with the Q-TOF mass spectrometer. The
192 ESI mass spectra of the CH$_3$OH/H$_2$O 1:1 HCl pH = 3 and
193 CH$_3$OH/H$_2$O 1:1 KHSO$_4$ pH = 3 D-fructose solutions, taken
194 as representative of all the investigated systems, are reported in
195 Figures 2 and 3, respectively.
196   The ESI mass spectrum of the HCl pH = 3 starting solution
197 (Figure 2a) is dominated by the ions at m/z 383 and 203,
198 corresponding to the [(D-fructose)$_2$]Na$^+$ and [D-fructose]Na$^+$
199 species characteristic of the starting reactive sugar bounded to
200 ubiquitous sodium cations.
201   Comparing this spectrum with that of the reaction products
202 obtained by rinsing the residue deposited after the electrospray
203 deposition of 1 mL of the solution (Figure 2b), a decrease in
204 the ions at m/z 383 and 203 was observed, attesting to the
205 extensive sugar decomposition. The main product generated
206 by the D-fructose microdroplets deposition reactions is the ion
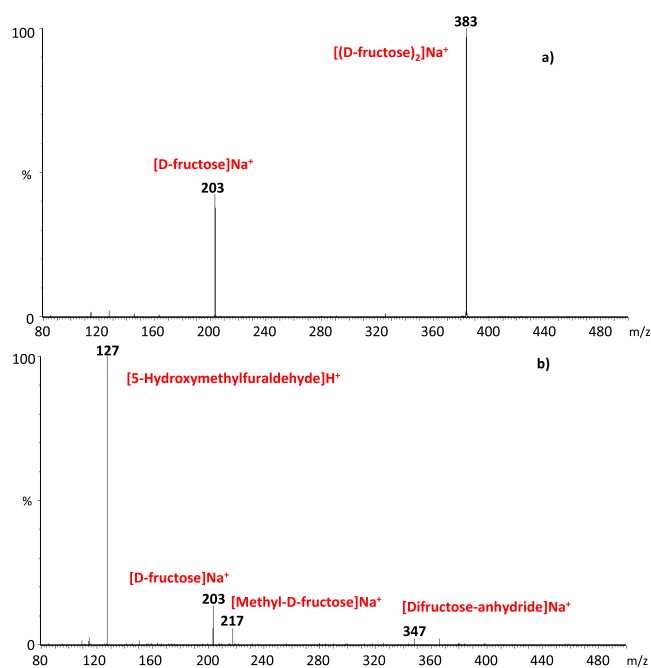207 at m/z 127 formally corresponding to protonated 5-HMF. The

Figure 2. ESI mass spectra of 10^{-3} M D-fructose CH$_3$OH/H$_2$O 1:1 (HCl) pH = 3 solutions: (a) zero-time ESI mass spectrum of the starting solution; (b) ESI mass spectrum of the solution obtained by rinsing the solid precipitate generated by the ESI deposition of 1 mL of the starting solution.
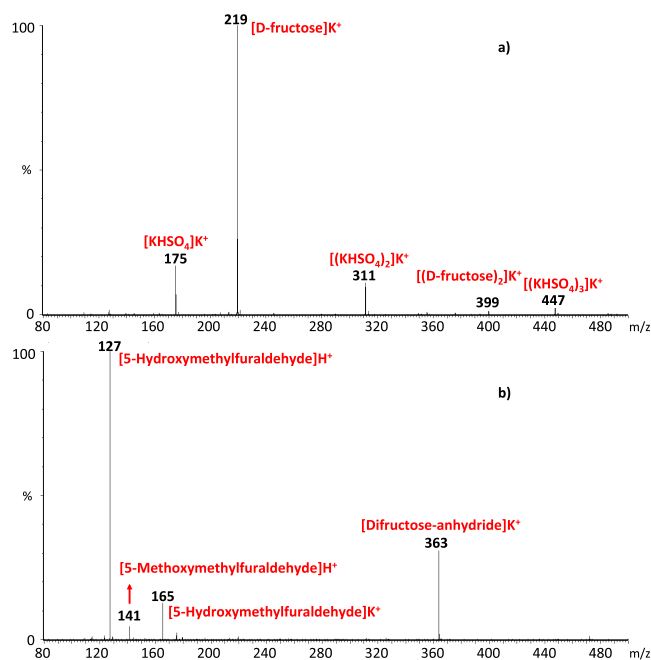

Figure 3. ESI mass spectra of 10^{-3} M D-fructose CH$_3$OH/H$_2$O 1:1 KHSO$_4$ pH = 3 solutions: (a) zero-time ESI mass spectrum of the starting solution; (b) ESI mass spectrum of the solution obtained by rinsing the solid precipitate generated by the ESI deposition of 1 mL of the starting solution.

208 D-fructose dimerization reaction leading to the formation of
209 difructose anhydrides is also catalyzed by HCl, as evidenced by
210 the formation of the [DFAs]Na$^+$ adduct at m/z 347. It is
211 interesting to underline the formation of the ionic product at
212 m/z 217, corresponding to sodiated methyl-D-fructose, that is

Table 1. D-Fructose Conversion Ratios Measured in Different Solvent Mixtures at a Desolvation Temperature of 200 °C

catalyst	pH	solvents	CR$^a_{dehydration}$	CR$^a_{dimerization}$	CR$^{a,b}_{methylation}$	total CR
HCl	3	H$_2$O	8.1			8.1
HCl	3	H$_2$O/CH$_3$CN 1:1	54.8	4.0		58.8
HCl	3	H$_2$O/CH$_3$OH 1:1	60.7	1.7	3.7	66.1
HCl	4	H$_2$O/CH$_3$OH 1:1				
KHSO$_4$	3	H$_2$O	51.1	42.2		93.3
KHSO$_4$	3	H$_2$O/CH$_3$CN 1:1	80.5	14.9		95.4
KHSO$_4$	3	H$_2$O/CH$_3$OH 1:1	72.0	22.3	4.9	99.2

^{a}CR denotes the ratio between the product ion intensity and reactant and byproduct ion intensity. ^{b}Methylation products refer to the sum of 5-methoxymethylfuraldehyde and methyl-D-fructose.

indicative of a peculiar microdroplets methylation reaction, reasonably due to the presence of methanol as cosolvent.

Moving to the KHSO$_4$ system, the spectrum of D-fructose/KHSO$_4$ pH = 3 CH$_3$OH/H$_2$O starting solution (Figure 3a) is dominated by an intense ion at m/z 219 that corresponds to the metal adduct between the potassium cation and D-fructose, whereas the minor ionic distribution of the type [K-(KHSO$_4$)$_n$]$^+$ ($n = 1-3$) at m/z 175, 311, and 447 can be ascribed to the molecular speciation characteristic of the inorganic salts in the gas phase.

As shown in Figure 3b, also the ESI mass spectrum of the solid obtained by the microdroplets deposition reaction catalyzed by KHSO$_4$ is dominated by the [5-HMF]H$^+$ ions at m/z 127 and [5-HMF]K$^+$ ions at m/z 165, characteristic of the D-fructose dehydration reaction. Methylation and dimerization reaction products are also present, as attested by the formation of the ion at m/z 141, corresponding to protonated 5-methoxymethylfuraldehyde, and the [DFAs]K$^+$ adduct at m/z 363. It is worth noting that, in this case, the methylation reaction seems to involve 5-HMF rather than the D-fructose starting reagent, as observed in the reaction catalyzed by HCl. To verify whether the methylation reaction occurs on D-fructose that subsequently dehydrates to form the ion at m/z 141 or the latter species derives by the direct methylation of 5-HMF, a CH$_3$OH/H$_2$O 1:1 KHSO$_4$ pH = 3 solution of 5-HMF was submitted to microdroplets deposition reaction under the same experimental conditions used for D-fructose. No methylated products were observed, thus demonstrating that D-fructose is methylated prior to undergoing the dehydration reaction leading to the ions at m/z 141. Evidently, KHSO$_4$ more efficiently catalyzes the dehydration of methylated D-fructose with respect to HCl.

The definitive attribution of reaction neutral products to 5-hydroxymethylfuraldehyde and 5-methoxymethylfuraldehyde was obtained by comparing the characteristic CID mass spectra of the ions at m/z 127 and m/z 141 with those of protonated standard molecules (Figures S1 and S2). The Na$^+$- and K$^+$-cationized DFAs ions at m/z 347 and 363, respectively, do not fragment by collision, thus suggesting the formation of strongly bound molecules, such as difructose anhydrides, rather than simple cation adducts between two 162 Da neutral moieties.

The ESI mass spectra of the recovered solutions obtained by rinsing the solid residue obtained after the microdroplets deposition clearly demonstrate that dehydration, methylation, and dimerization are the peculiar D-fructose reaction channels common to the two different inorganic acid catalysts used. To investigate the role of the solution composition on the branching ratios of these reaction channels, different solvent mixtures at different pH values were tested. Table 1 reports the conversion ratios of the three different processes measured starting from a pure water solution to H$_2$O/CH$_3$OH and H$_2$O/CH$_3$CN mixtures.

Among the systems catalyzed by HCl, the H$_2$O/CH$_3$OH 1:1 mixture at pH = 3 gives the higher sugar conversion ratio with the dehydration channel that strongly predominates over the methylation and dimerization reactions. Methylation disappears when the reaction is performed in H$_2$O/CH$_3$CN, whereas all the reaction channels are suppressed by using pure water. The lack of methylated products in the mixtures containing CH$_3$CN clearly underlines the role of methanol to promote the methylation reaction channel. No reactions were observed with HCl at pH values higher than 3 even at desolvation gas temperatures above 300 °C.

A total conversion ratio approaching 100% was measured for all the investigated mixtures involving KHSO$_4$ as an acid catalyst. The H$_2$O/CH$_3$CN solution at pH = 3 is the optimal system to catalyze the D-fructose dehydration with KHSO$_4$, whereas the dimerization reaction is increased under the conditions that seem to hinder the dehydration channel as in the case of a pure water solution.

By comparing all of the results, KHSO$_4$ seems to be the best catalyst to accelerate the D-fructose reactions by microdroplets deposition in the slightly acidic condition used (total CR = 99.2%). Moreover, the H$_2$O/CH$_3$OH pH = 3 systems containing HCl or KHSO$_4$, allowing the observation of more extensive D-fructose decomposition, were chosen as model solutions for the subsequent experiments.

Effects of the ESI Z-Spray Source Parameters. In previous studies concerning accelerated microdroplets reactions, the ESI source parameters were crucial in affecting the conversion ratio of the process under investigation.[41−43] Considering that the temperature strongly affects the D-fructose caramelization reaction, the influence of this parameter on the branching ratio between the observed reaction channels of the two D-fructose H$_2$O/CH$_3$OH pH = 3 model mixtures was first investigated. In the instrumental setup used in our experiment, the source block temperature does not influence the D-fructose reactivity since the microdroplets formed on the way from the ESI needle to the metal plate do not cross the MS inlet before being collected. On the contrary, the reaction outcome can be mainly affected by the temperature of the desolvation gas that promotes solvent evaporation both in the flying microdroplets and in the thin film resulting from their deposition onto the solid target. In the ESI Z-spray source, the nitrogen desolvation gas is heated and delivered as a coaxial sheath to the nebulized liquid spray by passing through a desolvation nozzle that can be heated up to 350 °C. The temperatures of the desolvation nozzle were varied from 50 to 350 °C and the corresponding actual spray

temperatures were measured by a thermocouple intercepting the microdroplets stream prior to their deposition onto the target (Figure S3). Commonly, the actual temperatures measured were around 50% of the set desolvation gas temperature, i.e., a desolvation gas temperature of 200 °C corresponds to an actual spray temperature of about 90 °C. In Figures 4 and 5, the relative intensities of the three reaction
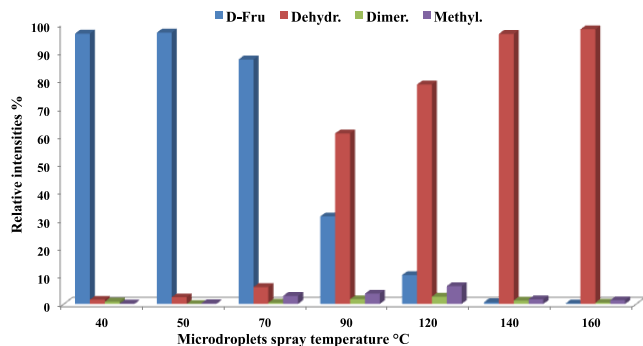

Figure 4. HCl-catalyzed reaction channel relative intensities (%) versus microdroplet spray temperatures (°C). Other source parameters are as follows: capillary 4 kV, pump flow 20 μL min^{-1}, and desolvation gas flow 200 L h^{-1}.
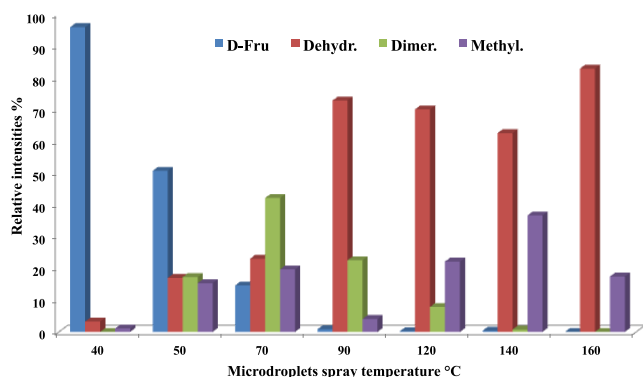

Figure 5. KHSO$_4$-catalyzed reaction channel relative intensities (%) versus microdroplets spray temperature (°C). Other source parameters are as follows: capillary 4 kV, pump flow 20 μL min^{-1}, and desolvation gas flow 200 L h^{-1}.

channels catalyzed by HCl and KHSO$_4$, respectively, are plotted as a function of the actual microdroplet spray measured temperatures.

By using HCl as a catalyst, the dehydration reaction (red bars) predominates over the other reaction channels at all the tested temperatures. The 5-HMF formation starts at a spray temperature around 90 °C and reaches a maximum relative intensity of about 100% at 140 °C.

The methylation and dimerization are minor side reaction channels that never overcame a relative intensity of 10%, with the methylation that has its maximum intensity at 120 °C.

As displayed in Figure 5, the D-fructose conversion catalyzed by KHSO$_4$ is already complete at a spray temperature of 90 °C, converse to the HCl system where a temperature of at least 140 °C is necessary to fully decompose the sugar.

The yield of 5-HMF in the KHSO$_4$ system progressively increases with the spray temperature up to a threshold value of ca. 90% at 160 °C. Moreover, a temperature around 90 °C is required to maximize the selectivity of the process toward the

dehydration reaction. The optimal temperature to drive the reaction to the production of DFAs is 70 °C, whereas the D-fructose methylation reaction starts at a temperature around 50 °C and reaches a maximum relative intensity of about 40% at 140 °C.

By comparing the graphics of the two different catalysts used, it is evident the stronger ability of KHSO$_4$ to promote all the D-fructose decomposition channels even at lower temperatures than HCl. The peculiar property of the HCl solution is the capability to drive the reaction almost completely to the selective formation of 5-HMF.

The ESI capillary voltage is another fundamental source parameter that typically influences the nature of the desolvation process leading to the microdroplets formation.[44,45] The relative intensities of the three different reaction channels were measured at a capillary voltage of 0 kV and at a spray temperature of 50 °C, at which the D-fructose is not fully decomposed, in order to determine whether this parameter influenced the observed reactions. Similar results were obtained in the absence of the applied capillary voltage with respect to the 4 kV capillary voltage experiments, thus demonstrating that the conversion ratios measured are only slightly affected by the ESI source electric field (Figure S4).

Microdroplets or Thin Films Reactions? To determine whether the reactions occur during the microdroplets flight to the target or by the fast evaporation of the thin film formed by their deposition onto the solid surface, the target surface was moved closer to the ESI source cone entrance (0.5 cm). At such a small distance, the microdroplets lifetime is too low to allow reactions and the spray composition reflects that of the starting mixture, as demonstrated by the starting solution spectra previously reported. As shown in Figure 6, the mass spectra of the solid residues recovered by spraying the D-
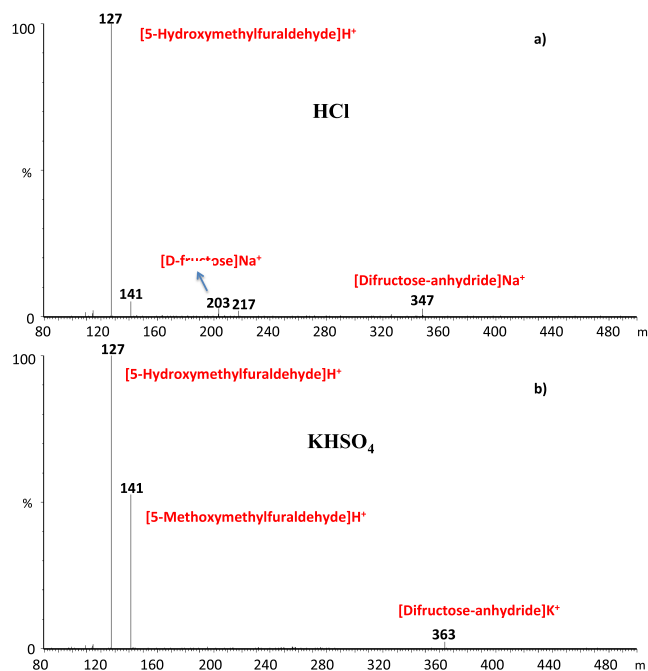

Figure 6. Mass spectrum of the solid residue obtained by spraying a 10^{-3} M D-fructose solution onto the solid target positioned at a 0.5 cm distance from the ESI tip: (a) H$_2$O/CH$_3$OH HCl 1:1 pH = 3 solution; (b) H$_2$O/CH$_3$OH 1:1 KHSO$_4$ pH = 3 solution. The measured spray temperature was 110 °C.

fructose model mixtures onto the solid surface positioned at the shortest distance from the ESI probe contain all the characteristic dehydration, dimerization and methylation ionic products already observed at the longer target distance.

This suggests that the observed reactions do not occur during the microdroplets flight toward the solid surface; rather, the recovered solid products derive from the rapid evaporation of the thin film of liquid produced by the microdroplets deposition. Moreover, this evidence explains the strong sensitivity of the reaction outcome to the spray temperature value and the lack of remarkable effects by changing the capillary voltage that influences only the microdroplets formation process.

Microdroplet Thin-Film Deposition versus Bulk Reactions. To establish the apparent acceleration factors of the reactions observed in the microdroplets thin films deposition process with respect to the same reactions in bulk, the same D-fructose H_2O/CH_3OH 1:1 pH = 3 solutions containing HCl or $KHSO_4$ were heated at 100 °C under reflux for 1 h, i.e., almost the same experimental conditions used to measure the conversion ratios reported in Table 1.

The spectra of the HCl solution taken at time zero and after 1 h of reaction are completely superimposable (Figure S5). None of the dehydration, dimerization, and methylation reactions occur in the HCl solution at pH = 3. Only a very low conversion ratio to 5-HMF was, instead, observed for the solution containing $KHSO_4$ as a catalyst (Figure S6).

D-Fructose dimerization and methylation reactions catalyzed by HCl and $KHSO_4$ at pH = 3 are peculiar reaction channels of the microdroplets thin film deposition process and do not occur in solution under the same experimental conditions. $KHSO_4$ catalyzes the dehydration reaction both in the thin-film system and in solution at pH = 3. Nevertheless, by considering the $KHSO_4$ dehydration conversion ratio of about 7.0% measured in bulk, an apparent acceleration factor of 10.5 can be estimated for the corresponding thin-film process.

CONCLUSIONS

The fast desolvation of D-fructose thin films generated by microdroplets deposition of HCl or $KHSO_4$ slightly acidic solutions onto a stainless-steel surface leads to the formation of D-fructose dehydration, methylation, and dimerization products, such as 5-hydroxymethylfuraldehyde, 5-methoxymethyl-furaldehyde, and difructose anhydrides. The reaction outcome is highly dependent on the catalyst and solvent employed as well as on the spray temperature value. It is interesting to note that a diluted solution of a "green" catalyst, such as $KHSO_4$, promotes the total conversion of the sugar at a spray temperature around 90 °C, whereas HCl selectively drives the reaction to the D-fructose dehydration under mild synthetic conditions by which the bulk reaction does not take place. The dimerization and methylation reactions catalyzed by $KHSO_4$ are peculiar to the thin-film system and do not occur in bulk, whereas $KHSO_4$-catalyzed dehydration is accelerated by an apparent factor of about 10.5 with respect to the same reaction in solution.

ASSOCIATED CONTENT

Ⓢ Supporting Information

The Supporting Information is available free of charge at https://pubs.acs.org/doi/10.1021/jasms.1c00363.

CID spectra of standard molecules compared with the CID spectra of the D-fructose microdroplets/thin film reaction products (Figures S1 and S2). Picture of the ESI Z-spray source adapted to spray/thin-film temperature measurements (Figure S3). Reaction channel relative intensities at 0 and 4 kV applied capillary voltage (Figure S4). ESI mass spectra of D-fructose HCl or $KHSO_4$ solutions heated at 100 °C under reflux (Figures S5 and S6) (PDF)

AUTHOR INFORMATION

Corresponding Authors

Federico Pepi — *Department of Chemistry and Drug Technologies, "Sapienza" University of Rome, 00185 Rome, Italy;* ⓘ orcid.org/0000-0001-6617-8192; Email: federico.pepi@uniroma1.it

Chiara Salvitti — *Department of Chemistry and Drug Technologies, "Sapienza" University of Rome, 00185 Rome, Italy;* Email: chiara.salvitti@uniroma1.it

Authors

Giulia de Petris — *Department of Chemistry and Drug Technologies, "Sapienza" University of Rome, 00185 Rome, Italy*

Anna Troiani — *Department of Chemistry and Drug Technologies, "Sapienza" University of Rome, 00185 Rome, Italy*

Marta Managò — *Department of Chemistry and Drug Technologies, "Sapienza" University of Rome, 00185 Rome, Italy*

Claudio Villani — *Department of Chemistry and Drug Technologies, "Sapienza" University of Rome, 00185 Rome, Italy;* ⓘ orcid.org/0000-0002-3253-3608

Alessia Ciogli — *Department of Chemistry and Drug Technologies, "Sapienza" University of Rome, 00185 Rome, Italy*

Andrea Sorato — *Department of Chemistry and Drug Technologies, "Sapienza" University of Rome, 00185 Rome, Italy*

Andreina Ricci — *Department of Mathematics and Physics, University of Campania L. Vanvitelli, 81100 Caserta, Italy;* ⓘ orcid.org/0000-0002-6172-0074

Complete contact information is available at:
https://pubs.acs.org/10.1021/jasms.1c00363

Author Contributions

F.P. conceived the idea, supervised the work, and wrote the original draft. C.S. and A.T. supervised the work and revised the original draft. C.S., M.M., A.C., and A.S. performed the experiments. The final version of the manuscript was written through the critical contributions of all the authors.

Notes

The authors declare no competing financial interest.

Rome University, for a postdoc position within the project Dipartimenti di Eccellenza-L. 232/2016.

■ REFERENCES

(1) Cooks, R. G.; Chen, H.; Eberlin, M. N.; Zheng, X.; Tao, W. A. Polar Acetalization and Transacetalization in the Gas Phase: The Eberlin Reaction. *Chem. Rev.* **2006**, *106*, 188−211.

(2) Eberlin, M. N. Electrospray Ionization Mass Spectrome-try: A Major Tool to Investigate Reaction Mechanisms in Both So-lution and the Gas Phase. *Eur. J. Mass Spectrom.* **2007**, *13*, 19−28.

(3) Salvitti, C.; Bortolami, M.; Chiarotto, I.; Troiani, A.; de Petris, G. The Knoevenagel reaction catalysed by ionic liquids: a mass spectrometric insight into the reaction mechanism. *New J. Chem.* **2021**, *45*, 17787−17795.

(4) Vikse, K. L.; McIndoe, J. S. Mechanistic insights from mass spectrometry: examination of the elementary steps of catalytic reactions in the gas phase. *Pure Appl. Chem.* **2015**, *87*, 361−377.

(5) Ray, A.; Bristow, T.; Whitmore, C.; Mosely, J. On-line reaction monitoring by mass spectrometry, modern approaches for the analysis of chemical reactions. *Mass Spec. Rev.* **2018**, *37*, 565−57.

(6) Iazzetti, A.; Mazzoccanti, G.; Bencivenni, G.; Righi, P.; Calcaterra, A.; Villani, C.; Ciogli, A. Primary Amine Catalyzed Activation of Carbonyl Compounds: A Study on Reaction Pathways and Reactive Intermediates by Mass Spectrometry. *Eur. J. Org. Chem.* **2022**, DOI: 10.1002/ejoc.202101272.

(7) Fenn, J. B.; Mann, M.; Meng, C. K.; Wong, S. F.; Whitehouse, C. M. Electrospray ionization for mass spectrometry of large biomolecules. *Science.* **1989**, *246*, 64−71.

(8) Yan, X.; Bain, R. M.; Cooks, R. G. Organic Reactions in Microdroplets: Reaction Acceleration Revealed by Mass Spectrom-etry. *Angew. Chem.* **2016**, *55*, 12960−12972.

(9) Salvitti, C.; Rosi, M.; Pepi, F.; Troiani, A.; de Petris, G. Reactivity of transition metal dioxide anions MO2- (M = Co, Ni, Cu, Zn) with sulfur dioxide in the gas phase: An experimental and theo-retical study. *Chem. Phys. Lett.* **2021**, *776*, 138555.

(10) Troiani, A.; Rosi, M.; Garzoli, S.; Salvitti, C.; de Petris, G. Iron-Promoted C-C bond formation in the gas phase. *Angew. Chem.* **2015**, *54*, 14359−14362.

(11) Troiani, A.; Salvitti, C.; de Petris, G. Gas-phase reactivi-ty of carbonate ions with sulphur dioxide: an experimental study of cluster reactions. *J. Am. Soc. Mass Spectrom.* **2019**, *30*, 1964−1972.

(12) Hou, J.; Zheng, Q.; Badu-Tawiah, A. K.; Xiong, C.; Guan, C.; Chen, S.; Nie, Z.; Wang, D.; Wan, L. Electrospray soft-landing for the construction of non-covalent molecular nanostruc-tures using charged droplets under ambient conditions. *Chem. Commun.* **2016**, *52*, 13660.

(13) Yan, X.; Bain, R. M.; Cooks, R. G. Organic reaction in microdroplets: reaction acceleration revealed by mass spectrometry. *Angew. Chem.* **2016**, *55*, 12960.

(14) Badu-Tawiah, A. K.; Cyriac, J.; Cooks, R. G. Reactions of organic ions at ambient surfaces in a solvent-free environment. *J. Am. Soc. Mass Spectrom.* **2012**, *23*, 842.

(15) Badu-Tawiah, A. K.; Campbell, D. I.; Cooks, R. G. Re-actions of microsolvated organic compounds at ambient surfaces: droplet velocity, charge state, and solvent effects. *J. Am. Soc. Mass Spectrom.* **2012**, *23*, 1077.

(16) Müller, T.; Badu-Tawiah, S. K.; Cooks, R. G. Accelerat-ed carbon-carbon bond-forming reactions in preparative elec-trospray. *Angew. Chem.* **2012**, *51*, 11832.

(17) He, Q.; Badu-Tawiah, A. K.; Chen, S.; Xiong, C.; Liu, H.; Zhou, Y.; Hou, J.; Zhang, N.; Li, Y.; Xie, X.; Wang, J.; Mao, L.; Nie, Z. In situ bioconjugation and ambient surface modification using reactive charged droplets. *Anal. Chem.* **2015**, *87*, 3144.

(18) Ansu-Gyeabourh, E.; Amoah, E.; Ganesa, C.; Badu-Tawiah, A. K. Monoacylation of symmetrical diamines in charge microdroplets. *J. Am. Soc. Mass Spectrom.* **2021**, *32*, 531.

(19) Huang, K. H.; Wei, Z.; Cooks, R. G. Accelerated reac-tions of amines with carbondioxide driven by superacid at the mi-crodroplet interface. *Chem. Sci.* **2021**, *12*, 2242.

(20) Zhao, P.; Gunawardena, H. P.; Zhong, X.; Zare, R. N.; Chen, H. Microdroplet ultrafast reactions speed antibody character-ization. *Anal. Chem.* **2021**, *93*, 3997.

(21) Wei, Z.; Wleklinski, M.; Ferreira, C.; Cooks, R. G. Reac-tion Acceleration in Thin Films with Continuous Product Deposi-tion for Organic Synthesis. *Angew. Chem.* **2017**, *56*, 9386−9390.

(22) Wei, Z.; Zhang, X.; Wang, J.; Zhang, S.; Zhang, X.; Cooks, R. G. High yield accelerated reactions in nonvolatile mi-crothin films: chemical derivatization for analysis of single-cell in-tracellular fluid. *Chem. Sci.* **2018**, *9*, 7779−7786.

(23) Wei, Z.; Li, Y.; Cooks, R. G.; Yan, X. Accelerated Reac-tion Kinetics in Microdroplets: Overview and Recent Deve-lopments. *Annu. Rev. Phys. Chem.* **2020**, *71*, 31−51.

(24) Pepi, F.; Ricci, S.; Garzoli, A.; Troiani, A.; Salvitti, C.; Di Rienzo, B.; Giacomello, P. A mass spectrometric study of the acid-catalysed D-fructose dehydration in the gas phase. *Carbohydr. Res.* **2015**, *413*, 145.

(25) Garzoli, S.; Antonini, L.; Troiani, A.; Salvitti, C.; Gia-Comello, P.; Patsilinakos, A.; Ragno, R.; Pepi, F. Gas-phase struc-tures and thermochemical properties of protonated 5-HMF isomers. *Int. J. Mass Spectrom.* **2020**, *447*, 116237.

(26) Troiani, A.; de Petris, G.; Pepi, F.; Garzoli, S.; Salvitti, C.; Rosi, M.; Ricci, A. Base-assisted conversion of protonated D-fructose to 5-HMF: searching for gas-phase green models. *Chem. Open.* **2019**, *8*, 1190.

(27) Antonini, L.; Garzoli, S.; Ricci, A.; Troiani, A.; Salvitti, C.; Giacomello, P.; Ragno, R.; Patsilinakos, A.; Di Rienzo, B.; Pepi, F. Ab-initio and experimental study of pentose sugar dehydration mechanism in the gas phase. *Carbohydr. Res.* **2018**, *19*, 458−459.

(28) Cimino, P.; Troiani, A.; Pepi, F.; Garzoli, S.; Salvitti, C.; Di Rienzo, B.; Barone, V.; Ricci, A. From ascorbic acid to furan derivatives: The gas phase acid catalyzed degradation of vitamin C. *Phys. Chem. Chem. Phys.* **2018**, *20*, 17132.

(29) Shrotri, A.; Kobayashi, H.; Fukuoka, A. Catalytic Con-version of Structural Carbohydrates and Lignin to Chemicals. *Ad-vances in Catalysis.* **2017**, *60*, 59−126.

(30) Mika, L. T.; Cséfalvay, E.; Németh, Á. Catalytic Con-version of Carbohydrates to Initial Platform Chemicals, Chemistry and Sustainability. *Chem. Rev.* **2018**, *118*, 505−613.

(31) Van Putten, R. J.; Van der Waal, J. C.; De Jong, E.; Rasrendra, C. B.; Heeres, H. J.; De Vries, J. G. Hydroxymethyl-furfural, a versatile platform chemical made from renewable re-sources. *Chem. Rev.* **2013**, *113*, 1499−1597.

(32) Wang, H.; Zhu, C.; Li, D.; Liu, Q.; Tan, J.; Wang, C.; Cai, C.; Ma, L. Recent advances in catalytic conversion of biomass to 5-hydroxymethylfurfural and 2, 5-dimethylfuran. *Renew. Sust. Energy Rev.* **2019**, *103*, 227−247.

(33) Yu, I. K.M.; Tsang, D. C.W. Conversion of biomass to hy-droxymethylfurfural: a review of catalytic systems and underlying mechanisms. *Bioresour. Technol.* **2017**, *238*, 716−732.

(34) Christian, T. J.; Manley-Harris, M.; Field, R. J.; Parker, B. A. Kinetics of Formation of Di-d-fructose Anhydrides during Thermal Treatment of Inulin. *J. Agric. Food Chem.* **2000**, *48*, 1823−37.

(35) Ortiz Cerda, I. E.; Thammavong, P.; Caqueret, V.; Porte, C.; Mabille, I.; Garcia Fernandez, J. M.; Santillan, M. M.; Havet, J.-L. Synthesis of Prebiotic Caramels Catalyzed by Ion-Exchange Resin Particles: Kinetic Model for the Formation of Di-d-fructose Anhydrides. *J. Agric. Food Chem.* **2018**, *66*, 1693−700.

(36) Audemar, M.; Atencio-Genes, L.; Mellet, C. O.; Jérôme, F.; Fernández, J. M. G.; De Oliveira Vigier, K. Carbon dioxide as a traceless caramelization promotor: preparation of prebiotic difruc-tose anhydrides (DFAs)-enriched caramels from D-fructose. *J. Agric. Food Chem.* **2017**, *65*, 6093−6099.

(37) Kikuchi, H.; Nagura, T.; Inoue, M.; Kishida, T.; Sakurai, H.; Yokota, A.; Asano, K.; Tomita, F.; Sayama, K.; Senba, Y. Phys-ical, Chemical and Physiological Properties of Difructose Anhy-dride III Produced from Inulin by Enzymatic Reaction. *J. Appl. Gly-cosci.* **2004**, *51*, 291−296.

623 (38) Mellet, C. O.; Fernández, J. M. G. Difructose dianhy-drides
624 (DFAs) and DFS-enriched products as functional foods. *Top. Curr.*
625 *Chem.* **2010**, *294*, 49−77.

626 (39) Salvitti, C.; Troiani, A.; Mazzei, F.; D'Agostino, C.; Zumpano,
627 R.; Baldacchini, C.; Bizzarri, A. R.; Tata, A.; Pepi, F. The use of a
628 commercial ESI Z-spray source for ambient ion soft landing and
629 microdroplet reactivity experiments. *Int. J. Mass Spec-trom.* **2021**, *468*,
630 116658.

631 (40) Kholiya, F.; Meena, R. R.; Doddabhimappa, R. G.; Adi-Murthy,
632 S.; Meena, R. An integrated effluent free process for the production of
633 5-hydroxymethyl furfural (HMF), levulinic acid (LA) and KNS-ML
634 from aqueous seaweed extract. *Carbohydr. Res.* **2020**, *490*, 107953.

635 (41) Banerjee, S.; Zare, R. N. Influence of inlet capillary temperature
636 on the microdroplet chemistry studied by mass spec-trometry. *J. Phys.*
637 *Chem. A* **2019**, *123*, 7704−7709.

638 (42) Basuri, P.; Gonzalez, L. E.; Morato, N. M.; Pradeep, T.; Cooks,
639 R. G. Accelerated microdroplet synthesis of benzimidazoles by
640 nucleophilic addition to protonated carboxylic acids. *Chem. Sci.* **2020**,
641 *11*, 12686−12694.

642 (43) Kebarle, P.; Tang, L. From ions in solution to ions in the gas
643 phase. *Anal. Chem.* **1993**, *65*, 972−986.

644 (44) Tang, K.; Gomez, A. Generation by electrospray of
645 monodisperse water droplets for targeted drug delivery by inhala-
646 tion. *J. Aerosol Sci.* **1994**, *25*, 1237−1249.

647 (45) Banerjee, S.; Zare, R. N. Syntheses of isoquinoline and
648 substituted quinolones in charged microdroplets. *Angew. Chem., Int.*
649 *Ed.* **2015**, *54*, 14795−14799.